An Efficient Marching-on-in-Degree Solution of Transient Multiscale EM Scattering Problems

Zi He, Ru-Shan Chen, *Senior Member, IEEE*, and Wei E. I. Sha, *Member, IEEE*

***Abstract*— A marching-on-in-degree (MOD)-based time-domain domain decomposition method is proposed to efficiently analyze the transient electromagnetic scattering from electrically large multiscale targets. The algorithm starts with an octree that divides the whole scattering target into several subdomains. Then using the equivalence principle algorithm, each subdomain is enclosed by an equivalence sphere (ES), where both the RWG and BoR spatial basis functions are employed to expand the unknown currents. The interactions of the near-field subdomains are directly calculated by the method of moments, while the far-field interactions can be converted into the interactions of corresponding ESs. This scheme implicitly satisfies the current continuity condition, and the convergence can be accelerated as well. By harnessing the rotational symmetry of the ESs, the computational resources are reduced significantly compared with the traditional MOD method. Several numerical examples are presented to demonstrate the accuracy and efficiency of the proposed algorithm.**

***Index Terms*— Electromagnetic (EM) scattering, equivalence principle algorithm (EPA), time-domain domain decomposition method.**

I. Introduction

RECENTLY, the multiscale electromagnetic (EM) scattering problem has been an important research topic in computational electromagnetics society. The multiscale problem is extremely challenging for traditional numerical methods because of the bad convergence. A lot of numerical techniques were proposed to solve the problems with a high efficiency [1]–[7].

On the other hand, the transient EM scattering problems have been paid more and more attention due to its rich application. The time-domain integral equation (TDIE) is widely used to analyze wideband EM responses from scatterers. There are two representative schemes for the TDIE, namely, the marching-on-in-time (MOT) scheme [8] and marching-on-in-degree (MOD) scheme [9]. A great number of strategies have been proposed to speed up the two schemes, such as the multilevel plane-wave time-domain algorithm [10], the time-domain adaptive integral method [11], the fast Fourier transform [12], the UV method [13], and the adaptive cross approximate algorithm [14]. Unfortunately, all the abovementioned methods cannot improve the convergence of the matrix equation, which will result in bad computational efficiency.

Manuscript received October 26, 2015; revised February 23, 2016; accepted April 25, 2016. Date of publication April 27, 2016; date of current version July 5, 2016. This work was supported in part by the Fundamental Research Funds for the Central Universities under Grant 30920140121004 and in part by the National Natural Science Foundation of China under Grant 61431006, Grant 61271076, Grant 61171041, and Grant 61371037. *(Corresponding author: Ru-Shan Chen.)*

Z. He and R.-S. Chen are with the School of Electrical Engineering and Optical Technique, Nanjing University of Science and Technology, Nanjing 210094, China (e-mail: 15850554055@163.com; eerschen@njust.edu.cn).

W. E. I. Sha is with the University of Hong Kong, Pok Fu Lam, Hong Kong (e-mail: wsha@eee.hku.hk).

Color versions of one or more of the figures in this paper are available online at http://ieeexplore.ieee.org.

Digital Object Identifier 10.1109/TAP.2016.2559521

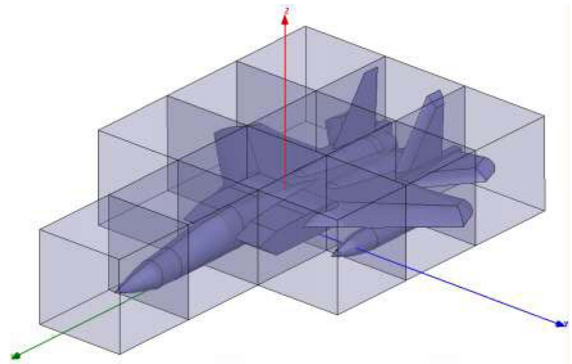

Fig. 1. 3-D grouping sketch for an airplane (nonzero subdomains).

In this paper, we proposed an efficient MOD solution to the transient multiscale EM scattering problems. First, the whole scattering target is divided into several subdomains with an octree data structure and each subdomain is enclosed by an equivalence sphere (ES). Then the interactions between two near-field subdomains are directly computed with the method of moments (MoM), while the far-field interactions can be replaced by the interactions of their corresponding ESs using the equivalence principle algorithm (EPA). It should be noted that the current continuity condition can be implicitly satisfied by this technique. Using the rotationally symmetric property of the ESs, the computational resources are reduced significantly [15]–[18]. Moreover, the basis transformation technique is adopted between the Rao-Wilton-Glisson (RWG) and body of revolution (BoR) basis sets defined on the ESs. Finally, both the inner iteration in each local subdomain and the outer iterations of all the subdomains are simultaneously employed to solve the whole system with a high convergence rate.

The remainder of this paper is organized as follows. The proposed algorithm is described in detail in Section II. In Section III, a series of numerical examples is given to demonstrate the accuracy and efficiency of the proposed method. Finally, the conclusion is given in Section IV.

II. Theory and Formulas

A. Grouping Implementation

As shown in Fig. 1, a cube is used to enclose the PEC airplane and the cube can be recursively decomposed into

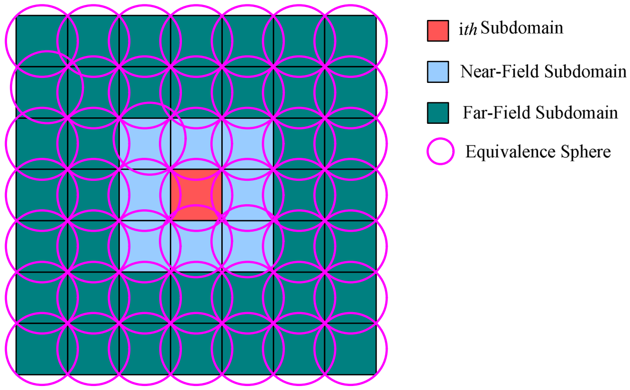

Fig. 2. 2-D grouping sketch.

eight subcubes. More specifically, a scattering target can be divided into several subdomains depending on an octree.

Each subdomain is enclosed with an ES with the same size. As shown in Fig. 2, the subdomains are defined as the near-field interaction when their ESs are overlapping with each other. Otherwise, they are the far-field interaction.

Suppose that a PEC target is illuminated by a plane wave in free space and it is divided into M subdomains, and the interaction in the ith subdomain can be calculated as

$$\begin{aligned}\mathbf{Z}_{ii}\mathbf{I}_i &= \mathbf{V}_i^{\text{inc}} + \sum_{j\in\Gamma_n}\mathbf{V}_{ij}^n + \sum_{j\in\Gamma_f}\mathbf{V}_{ij}^f \\ &= \mathbf{V}_i^{\text{inc}} + \sum_{j\in\Gamma_n}\mathbf{Z}_{ij}\mathbf{I}_j + \sum_{j\in\Gamma_f}\mathbf{Z}_{ij}\mathbf{I}_j \end{aligned} \tag{1}$$

where $\mathbf{Z}_{ii}$ is the self-acting matrix of the ith subdomain, $\mathbf{I}_i$ and $\mathbf{I}_j$ represent the unknown current coefficients for the ith and jth subdomains, respectively, $\mathbf{Z}_{ij}$ denotes the interaction matrix between the ith and jth subdomains, $\mathbf{V}_i^{\text{inc}}$ is the incident field for the ith subdomain, and Γ_n and Γ_f represent the near-field and far-field subdomains.

For near-field interactions, the RWG basis functions on the scattering target are directly calculated with the MoM. Then the induced electric field of the ith subdomain can be expressed in terms of the scattered electric current of the jth near-field subdomain

$$\begin{aligned}\mathbf{V}_{ij}^n(\mathbf{r},\tau) = \mathbf{Z}_{ij}\mathbf{I}_j &= -\frac{\mu_0}{4\pi}\frac{\partial}{\partial t}\int_S \frac{\mathbf{J}_{\text{PEC},j}^s(\mathbf{r}',\tau-R/c)}{R}dS \\ &\quad + \frac{\nabla}{4\pi\varepsilon_0}\int_S\int_{-\infty}^{\tau-R/c}\frac{\nabla'\cdot\mathbf{J}_{\text{PEC},j}^s(\mathbf{r}',\tau)}{R}d\tau dS \\ &\quad j\in\Gamma_n,\ \ \mathbf{r}\in i\text{th subdomain},\ \ \mathbf{r}'\in j\text{th subdomain}.\end{aligned} \tag{2}$$

However, the interactions of any two far-field subdomains are calculated by the ones between their corresponding ESs using the EPA [3], [22], [23]. In this way, the current continuity condition can be satisfied without tapping the basis functions. There are four steps for the calculation, namely, outside-in propagation, solving for the current on the object, inside-out propagation, and translation operator.

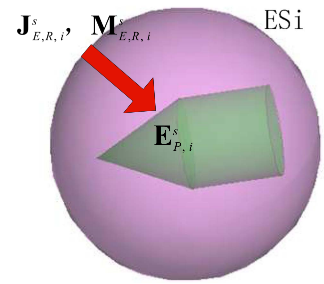

Fig. 3. Outside-in propagation process.

B. Outside-In Propagation

The scattered electric current on the scattering target is discretized with the RWG spatial basis functions [1] and the weighted Laguerre polynomial as the temporal basis functions [9]

$$\mathbf{J}_{\text{PEC},i}^s(\mathbf{r},\tau) = \sum_{n=1}^{N_s}\sum_{v=0}^{N_l}\{I_{\text{PEC},n,v,i}\mathbf{f}_n(\mathbf{r})\varphi_v(s\tau)\} \tag{3}$$

where PEC stands for the perfect electric conductor, $I_{\text{PEC},n,v,i}$ is the expansion coefficients of scattered electric current on the scattering target for basis function n and order v in the ith subdomain, $\mathbf{f}_n(\mathbf{r})$ denotes the spatial RWG basis functions, $\varphi_v(s\tau)$ is served as the temporal basis functions, and N_s and N_l represent the number of spatial and temporal basis functions, respectively.

The equivalent scattered electric/magnetic currents on ith ES are expanded as the RWG spatial basis functions, which can be written as

$$\mathbf{J}_{\text{ES,RWG},i}^s(\mathbf{r},\tau) = \sum_{n=1}^{N_s}\sum_{v=0}^{N_l}\left\{I_{\text{ES},n,v,i}^J\mathbf{f}_n(\mathbf{r})\varphi_v(s\tau)\right\} \tag{4}$$

$$\mathbf{M}_{\text{ES,RWG},i}^s(\mathbf{r},\tau) = \sum_{n=1}^{N_s}\sum_{v=0}^{N_l}\left\{I_{\text{ES},n,v,i}^M\mathbf{f}_n(\mathbf{r})\varphi_v(s\tau)\right\} \tag{5}$$

where ES stands for ES. $I_{\text{ES},n,v,i}^J$, and $I_{\text{ES},n,v,i}^M$ are the RWG expansion coefficients.

As shown in Fig. 3, the induced electric field on the scattering target for the ith subdomain that is illuminated by the source on the ith ES can be calculated as

$$\begin{aligned}\mathbf{E}_{\text{PEC},i}^s(\mathbf{r},\tau) = \frac{\mu_0}{4\pi}\frac{\partial}{\partial t}\int_S &\frac{\mathbf{J}_{\text{ES,RWG},i}^s(\mathbf{r}',\tau-R/c)}{R}dS \\ &- \frac{\nabla}{4\pi\varepsilon_0}\int_S\int_{-\infty}^{\tau-R/c}\frac{\nabla'\cdot\mathbf{J}_{\text{ES,RWG},i}^s(\mathbf{r}',\tau)}{R}d\tau dS \\ &- \frac{1}{4\pi}\int_S\nabla\times\frac{\mathbf{M}_{\text{ES,RWG},i}^s(\mathbf{r}',\tau)}{R}dS\end{aligned} \tag{6}$$

where $R = |\mathbf{r}-\mathbf{r}'|$, and ε_0 and μ_0 are, respectively, the permittivity and permeability in free space.

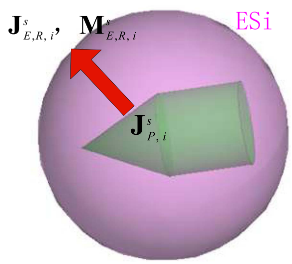

Fig. 4. Inside-out propagation process.

C. Solving for the Current on the Object

The scattered electric current on the PEC scattering target for the ith subdomain can be computed as

$$[\mathbf{E}^s_{\mathrm{PEC},i}(\mathbf{r},\tau)]_{\tan} = \left[\begin{array}{l} \dfrac{\mu_0}{4\pi}\dfrac{\partial}{\partial t}\displaystyle\int_S \dfrac{\mathbf{J}^{\mathrm{sca}}_{\mathrm{PEC},i}(\mathbf{r}',\tau-R/c)}{R}dS \\ -\dfrac{\nabla}{4\pi\varepsilon_0}\displaystyle\int_S\int_{-\infty}^{\tau-R/c}\dfrac{\nabla'\cdot\mathbf{J}^{\mathrm{sca}}_{\mathrm{PEC},i}(\mathbf{r}',\tau)}{R}d\tau dS \end{array}\right]_{\tan}. \tag{7}$$

D. Inside-Out Propagation

As shown in Fig. 4, the induced equivalent scattered electric/magnetic current on ith ES is obtained

$$\mathbf{J}^s_{\mathrm{ES,RWG},i}(\mathbf{r},\tau) = \hat{n}(\mathbf{r})\times\frac{1}{4\pi}\int_S\nabla\times\frac{\mathbf{J}^s_{\mathrm{PEC},i}(\mathbf{r}',\tau)}{R}dS \tag{8}$$

$$\mathbf{M}^s_{\mathrm{ES,RWG},i}(\mathbf{r},\tau) = \hat{n}(\mathbf{r})\times\left\{\begin{array}{l} \dfrac{\mu_0}{4\pi}\dfrac{\partial}{\partial t}\displaystyle\int_S\dfrac{\mathbf{J}^s_{\mathrm{PEC},i}(\mathbf{r}',\tau-R/c)}{R}dS \\ -\dfrac{\nabla}{4\pi\varepsilon_0}\displaystyle\int_S\int_{-\infty}^{\tau-R/c}\dfrac{\nabla'\cdot\mathbf{J}^s_{\mathrm{PEC},i}(\mathbf{r}',\tau)}{R}d\tau dS \end{array}\right\} \tag{9}$$

where $\hat{n}(\mathbf{r})$ is the outward normal unit vector of the ith ES.

E. Translation Operator

For the translation operator, the BoR basis functions [19]–[21] are used to discretize the ES and can be expressed as

$$\mathbf{J}^s_{\mathrm{ES,BoR},i}(\mathbf{r},\tau) = \sum_{\alpha=-\mathrm{Mod}}^{\mathrm{Mod}}\sum_{n=1}^{N_s}\sum_{v=0}^{N_l}\left\{\left[\begin{array}{l} I^{J,t}_{\mathrm{ES},\alpha,n,v,i}\mathbf{f}^t_{\alpha,n}(\mathbf{r}) \\ +I^{J,\varphi}_{\mathrm{ES},\alpha,n,v,i}\mathbf{f}^\varphi_{\alpha,n}(\mathbf{r})\end{array}\right]\varphi_v(s\tau)\right\} \tag{10}$$

$$\mathbf{M}^s_{\mathrm{ES,BoR},i}(\mathbf{r},\tau) = \sum_{\alpha=-\mathrm{Mod}}^{\mathrm{Mod}}\sum_{n=1}^{N_s}\sum_{v=0}^{N_l}\left\{\left[\begin{array}{l} I^{M,t}_{E,\alpha,n,v,i}\mathbf{f}^t_{\alpha,n}(\mathbf{r}) \\ +I^{M,\varphi}_{E,\alpha,n,v,i}\mathbf{f}^\varphi_{\alpha,n}(\mathbf{r})\end{array}\right]\varphi_v(s\tau)\right\} \tag{11}$$

where $I^{J,t}_{\mathrm{ES},\alpha,n,v,i}$, $I^{M,t}_{\mathrm{ES},\alpha,n,v,i}$, $I^{J,\varphi}_{\mathrm{ES},\alpha,n,v,i}$, and $I^{M,\varphi}_{\mathrm{ES},\alpha,n,v,i}$ are the BoR expansion coefficients of the ith ES for mode α, basis function n, and order v. $\mathbf{f}^t_{\alpha,n}(\mathbf{r})$ and $\mathbf{f}^\varphi_{\alpha,n}(\mathbf{r})$ denote the spatial basis functions in the longitudinal and azimuthal directions, respectively.

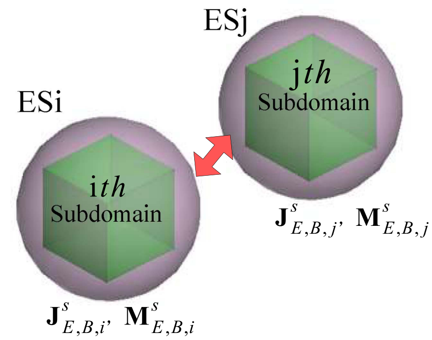

Fig. 5. Interaction between two far-field subdomains.

Therefore, the RWG-based electric/magnetic currents on ith ES should be converted into the BoR-based ones. Moreover, the coordinate transformation technique is adopted to transform the current coefficients among two different coordinate systems [22]

$$\left\langle\mathbf{J}^s_{\mathrm{ES,BoR},i}(\mathbf{r},\tau),\mathbf{f}^\gamma_{\alpha,n}(\mathbf{r})\right\rangle = \left\langle\mathbf{J}^s_{\mathrm{ES,RWG},i}(\mathbf{r},\tau),\mathbf{f}^\gamma_{\alpha,n}(\mathbf{r})\right\rangle \tag{12}$$

$$\left\langle\mathbf{M}^s_{\mathrm{ES,BoR},i}(\mathbf{r},\tau),\mathbf{f}^\gamma_{\alpha,n}(\mathbf{r})\right\rangle = \left\langle\mathbf{M}^s_{\mathrm{ES,RWG},i}(\mathbf{r},\tau),\mathbf{f}^\gamma_{\alpha,n}(\mathbf{r})\right\rangle \tag{13}$$

where $\gamma = t, \varphi$, $\langle,\rangle$ represents the inner-product operation.

Similarly, the BoR-based induced equivalent scattered electric/magnetic currents can also be converted into the RWG-based currents using the following equations:

$$\left\langle\mathbf{J}^s_{\mathrm{ES,RWG},i}(\mathbf{r},\tau),\mathbf{f}_n(\mathbf{r})\right\rangle = \left\langle\mathbf{J}^s_{\mathrm{ES,BoR},i}(\mathbf{r},\tau),\mathbf{f}_n(\mathbf{r})\right\rangle \tag{14}$$

$$\left\langle\mathbf{M}^s_{\mathrm{ES,RWG},i}(\mathbf{r},\tau),\mathbf{f}_n(\mathbf{r})\right\rangle = \left\langle\mathbf{M}^s_{\mathrm{ES,BoR},i}(\mathbf{r},\tau),\mathbf{f}_n(\mathbf{r})\right\rangle. \tag{15}$$

Suppose that the ith and jth subdomains are far-field interactions, as shown in Fig. 5. The interactions of two far-field subdomains can be computed as follows:

$$\begin{aligned}\mathbf{J}^s_{\mathrm{ES,BoR},i}(\mathbf{r},\tau) &= -\hat{n}(\mathbf{r})\times\frac{1}{4\pi}\int_S\nabla\times\frac{\mathbf{J}^s_{\mathrm{ES,BoR},j}(\mathbf{r}',\tau)}{R}dS+\frac{1}{\eta^2}\hat{n}(\mathbf{r}) \\ &\quad\times\left\{\begin{array}{l}\dfrac{\mu_0}{4\pi}\dfrac{\partial}{\partial t}\displaystyle\int_S\dfrac{\mathbf{M}^s_{\mathrm{ES,BoR},j}(\mathbf{r}',\tau-R/c)}{R}dS \\ -\dfrac{\nabla}{4\pi\varepsilon_0}\displaystyle\int_S\int_{-\infty}^{\tau-R/c}\dfrac{\nabla'\cdot\mathbf{M}^s_{\mathrm{ES,BoR},j}(\mathbf{r}',\tau)}{R}d\tau dS\end{array}\right\}\end{aligned} \tag{16}$$

$$\begin{aligned}\mathbf{M}^s_{\mathrm{ES,BoR},i}(\mathbf{r},\tau) &= -\hat{n}(\mathbf{r})\times\frac{1}{4\pi}\int_S\nabla\times\frac{\mathbf{M}^s_{\mathrm{ES,BoR},j}(\mathbf{r}',\tau)}{R}dS-\hat{n}(\mathbf{r}) \\ &\quad\times\left\{\begin{array}{l}\dfrac{\mu_0}{4\pi}\dfrac{\partial}{\partial t}\displaystyle\int_S\dfrac{\mathbf{J}^s_{\mathrm{ES,BoR},j}(\mathbf{r}',\tau-R/c)}{R}dS \\ -\dfrac{\nabla}{4\pi\varepsilon_0}\displaystyle\int_S\int_{-\infty}^{\tau-R/c}\dfrac{\nabla'\cdot\mathbf{J}^s_{\mathrm{ES,BoR},j}(\mathbf{r}',\tau)}{R}d\tau dS\end{array}\right\}.\end{aligned} \tag{17}$$

For the far-field interactions, the unknowns are expanded with spatial basis functions defined on the boundary curve and Fourier series in the azimuthal direction due to the rotationally

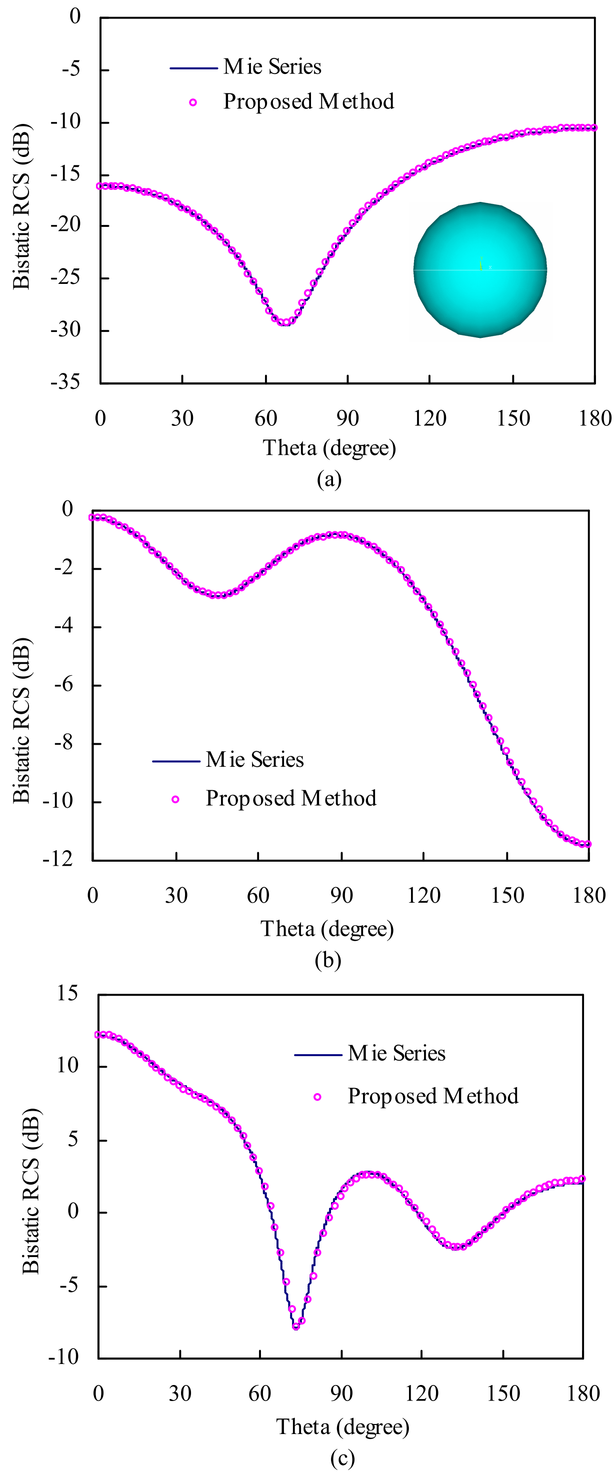

Fig. 6. Bistatic RCS results of a PEC sphere. (a) $f = 50$ MHz. (b) $f = 150$ MHz. (c) $f = 250$ MHz.

symmetric property of the ES. Therefore, both the memory requirement and the CPU time can be reduced significantly. It should be noted that the outer iteration among the far-filed subdomains is finished when the induced scattered electric current on the scattering target becomes stable.

III. Numerical Examples

In this section, several numerical results are presented to demonstrate the effectiveness of the proposed solver.

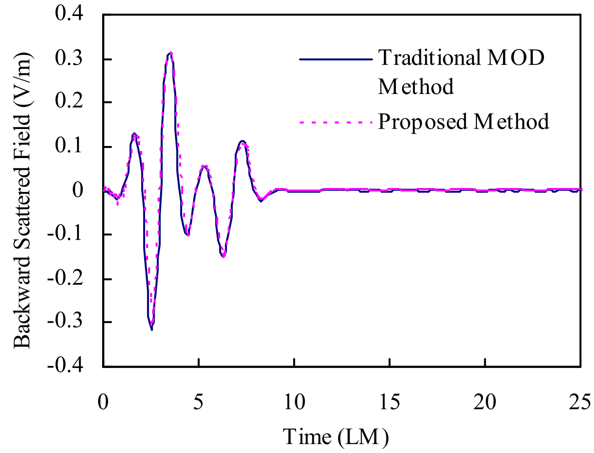

Fig. 7. Backward scattered field for a PEC sphere.

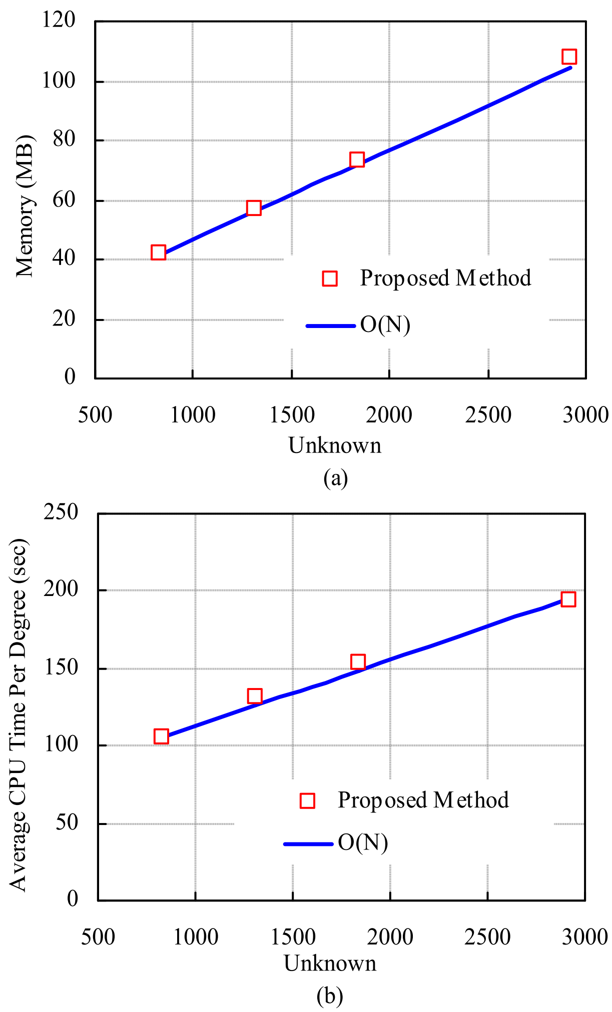

Fig. 8. (a) Memory requirement of PEC sphere versus spatial unknowns. (b) Average CPU time per degree of PEC sphere versus spatial unknowns.

All numerical results are tested on a Dell workstation with 40 CPUs and 512-GB memory. The mesh sizes of both the RWG and BoR basis functions for the ES are $0.1\lambda_{\min}$, where $\lambda_{\min}$ is the wavelength at the maximum frequency.

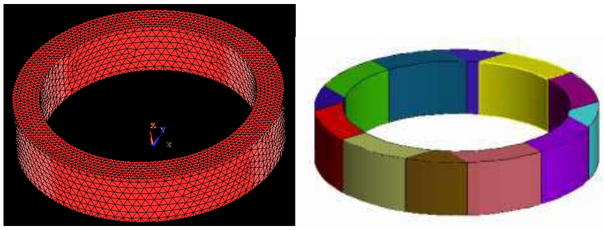

Fig. 9. (a) Meshes of the ring. (b) Grouping of the ring (one color stands for one group).

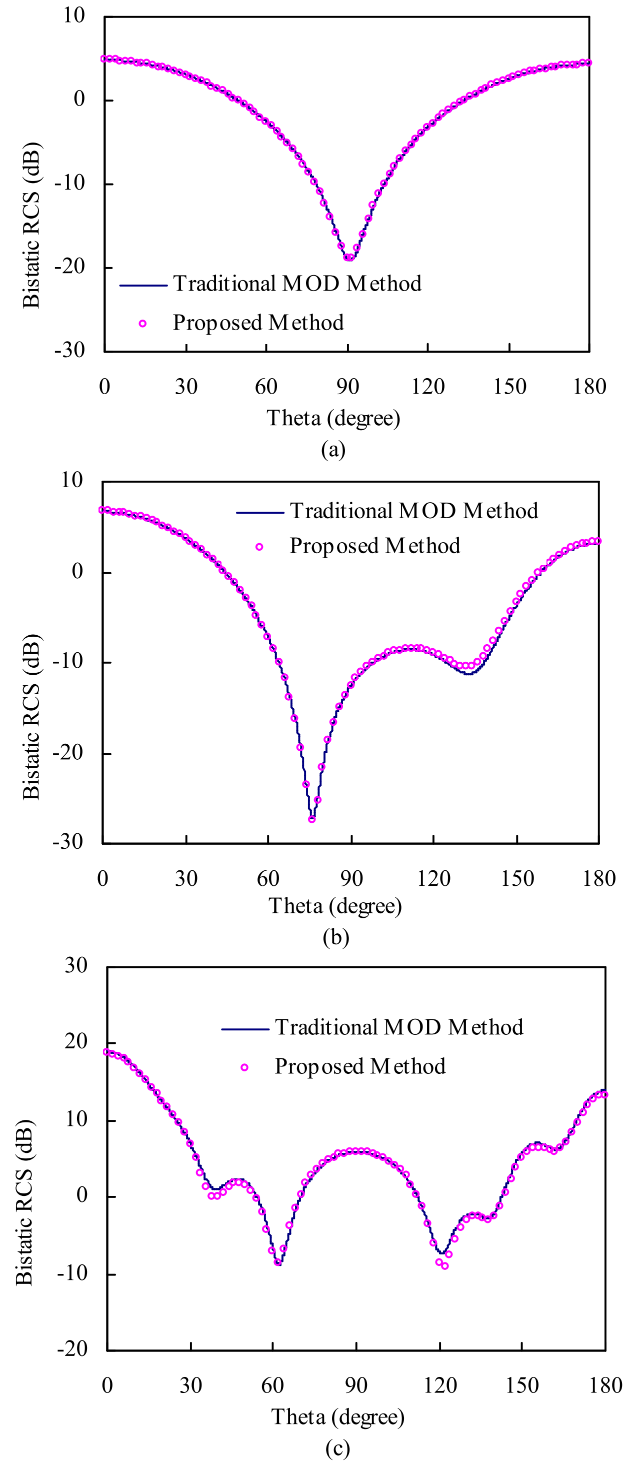

Fig. 10. Bistatic RCS results of the ring. (a) $f = 50$ MHz. (b) $f = 150$ MHz. (c) $f = 250$ MHz.

The incident wave is a modulated Gaussian pulse and is defined as

$$\mathbf{E}^{\mathbf{i}}(\mathbf{r}, t) = \hat{\mathbf{x}} \cos[2\pi f_0(t - R/c)] \cdot \exp\left[-\frac{(t - R/c - t_p)^2}{2\sigma^2}\right] \quad (18)$$

where f_0 is the center frequency, $\sigma = 6/(2\pi f_{\text{bw}})$, f_{bw} represents the bandwidth of the Gaussian impulse, and t_p is the time delay.

A. Accuracy and Computational Complexity

First, the transient EM scattering from a PEC sphere with a radius of 0.7 m is investigated with a center frequency of 150 MHz and a pulsewidth of 300 MHz. The incident plane wave is fixed at $\theta^{\text{inc}} = 0°$, $\varphi^{\text{inc}} = 0°$, and the time delay of the modulated Gaussian pulse is 4.5 lm. The mesh size for this sphere is 0.1 m. The unknown scattered electric current on the PEC sphere is expanded with 1836 spatial basis functions and 50 temporal basis functions. The whole computational domain is divided into 64 subdomains with a size of 0.4 m × 0.4 m × 0.4 m. It should be noted that there are 48 nonempty subdomains. Each of them is enclosed with an ES with a radius of 0.4 m. Each ES is discretized into 606 RWG and 16 BoR spatial basis functions. Four Fourier modes are needed in this computation. As shown in Fig. 6, the bistatic RCS results are compared between the proposed method and the Mie series at several frequencies. It can be seen that there is a good agreement between them. Moreover, the backward scattered field for the proposed method is compared with the one of the traditional MOD method in Fig. 7.

In addition, the computational complexity of the proposed method is investigated. Only the zeroth degree of the temporal basis function is simulated for the sake of available memory. Both the memory requirement and average CPU time per degree with 825, 1311, 1836, and 2919 spatial unknowns are shown in Fig. 8. It can be seen that the complexity of the proposed method scales as $O(N)$.

B. Convergence Performance and Optimal Grouping Scheme

Second, we consider the transient EM scattering from a ring with an inner radius of 1.2 m and an outer radius of 1.5 m. The time delay of the modulated Gaussian pulse is set to be 4.0 lm with a center frequency of 150 MHz and a pulsewidth of 300 MHz, where lm represents light meter and 1(lm) = 1/3.0e8. In this numerical example, 12 132 spatial basis functions and 80 temporal basis functions are adopted with four modal equations to be solved. The whole computational domain is divided into 64 subdomains with a size of 0.8 m × 0.8 m × 0.8 m, and there are 12 nonempty subdomains. The radius of the ES is 0.75 m, and the ES is discretized into 639 RWG and 24 BoR spatial basis functions. The meshes and the grouping of the ring are shown in Fig. 9.

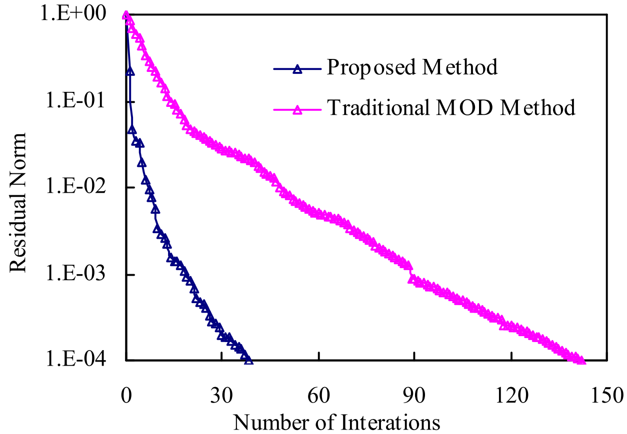

Fig. 11. Convergence history of the first order for the ring.

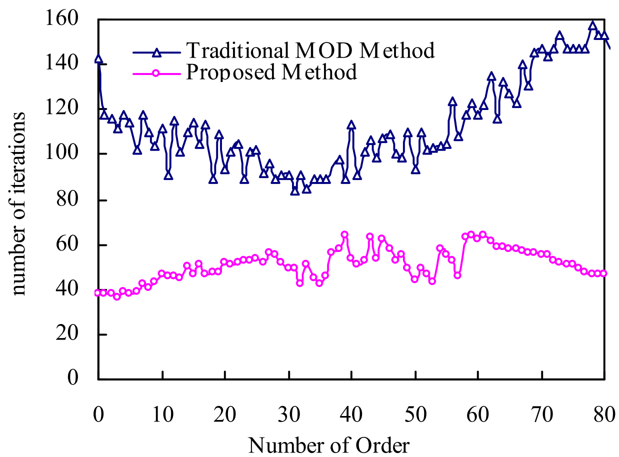

Fig. 12. Number of iterations versus temporal order.

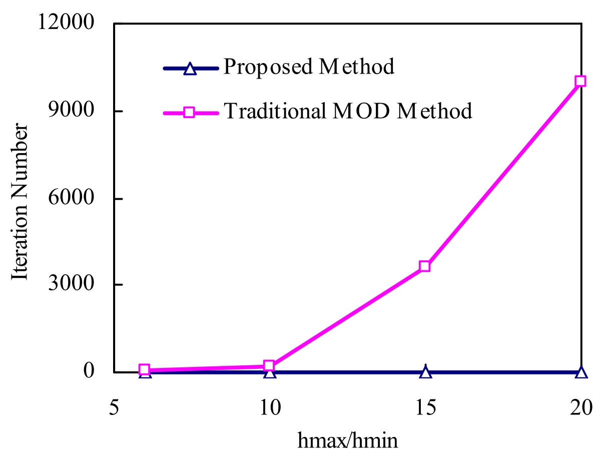

Fig. 13. Iteration number versus the ratio of the maximum mesh size over the minimum mesh size.

The mesh size of $0.05\lambda_{\min}$ is adopted to both the top and the down faces and $0.08\lambda_{\min}$ for the sides. As shown in Fig. 10, bistatic RCS results of the proposed method at several frequencies are given and compared with the traditional MOD method.

Moreover, the convergences for the first order are compared between them in Fig. 11, and the numbers of convergence for each order are given in Fig. 12. In addition, the convergence performance is tested for the multiscale problem. The part of the ring is meshed densely. As shown in Fig. 13, the iteration number of the proposed method is compared with the traditional MOD method versus the ratio of the maximum mesh size over the minimum mesh size. It can be found that the proposed method is much more stable for the multiscale problems.

Finally, the computational resources for different grouping schemes are given in Table I. The memory requirement can be reduced with the size of subdomains decreasing. However, more CPU time is needed when the grouping size is too small or too big. Some additional propagation operators are needed to be calculated when the grouping size is big, which will result in bad efficiency. On the other hand, a lot of CPU time is needed for the calculation of translation operators when the grouping size is small. It can be concluded from the numerical results that higher efficiency can be obtained when there is a good balance between the numbers of near-field and far-field interactions. Generally speaking, the optimal grouping scheme can be achieved when the number of BoR unknowns on the ES is much smaller than the one of RWG unknowns on the scattering target in this subcube and the total number of nonempty subdomains is less than 30 at the same time.

TABLE I
COMPARISONS OF DIFFERENT GROUPING SCHEMES

Size of Sub-domains (m)	No. of Sub-domains (Total/Nonempty)	Total CPU Time (h)	Memory Requirement (GB)
2.8	8/4	12.5	39.7
1.5	64/12	8.22	32.9
0.8	512/88	49.3	15.4

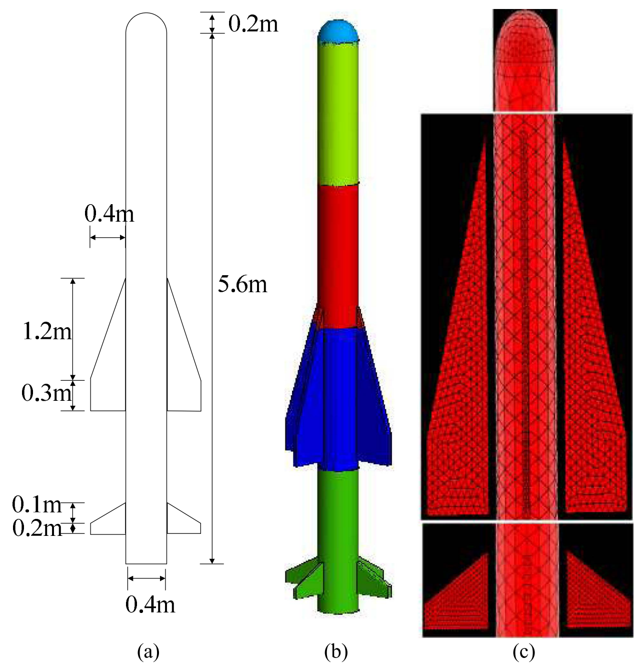

Fig. 14. (a) Geometry of the missile model. (b) Grouping of the missile model (one color stands for one group). (c) Mesh of the missile model.

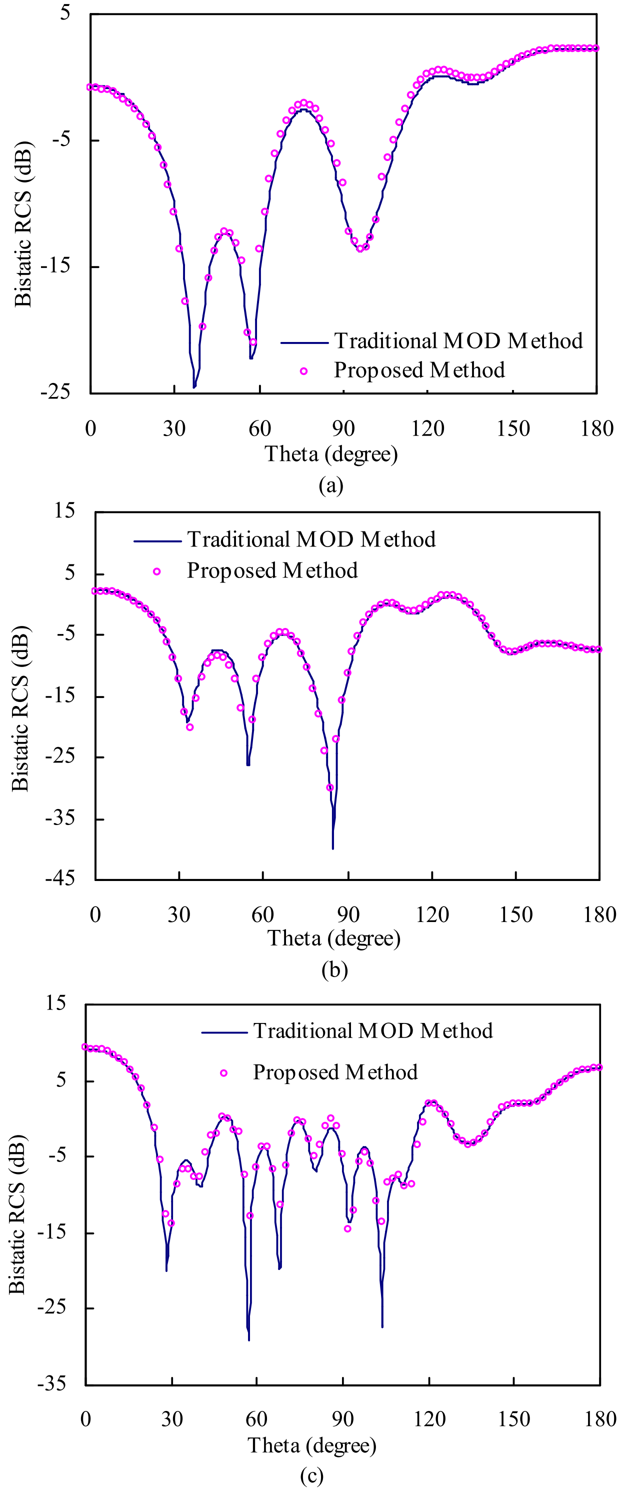

Fig. 15. Bistatic RCS results of the missile model. (a) $f = 50$ MHz. (b) $f = 150$ MHz. (c) $f = 250$ MHz.

C. Computational Efficiency

Third, a missile model is analyzed by the proposed method with the incident plane wave fixed at $\theta^{\mathrm{inc}} = 0°$ and $\varphi^{\mathrm{inc}} = 0°$. The geometry, the grouping scheme, and the mesh of the missile model are given in Fig. 14. It can be seen that the meshes are nonuniform on the surface. The mesh size of 0.1 m is adopted to the cylinder and 0.04 m for the wings.

TABLE II
COMPARISON OF THE AVERAGE NUMBER OF ITERATIONS, MEMORY REQUIREMENT, AND THE TOTAL CPU TIME FOR THE MISSILE MODEL

Methods	Average Number of Iteration	Memory Requirement (GB)	Total CPU Time (h)
Traditional MOD Method	602	197.8	17.8
Proposed Method	8	32.1	13.1

In this numerical example, the center frequency of modulated Gaussian pulse is 150 MHz, the pulsewidth is 300 MHz, and the time delay is 5.0 lm. This problem is discretized into 18 213 spatial basis functions and 80 temporal basis functions, and two Fourier modes are needed. The whole computational domain is divided into 512 subdomains with a size of 1.4 m $\times$ 1.4 m $\times$ 1.4 m, and there are five nonempty subdomains. The radius of the ES is 1.3 m, and the ES is discretized into 1329 RWG and 36 BoR spatial basis functions. As shown in Fig. 15, bistatic RCS results at several frequencies are compared between the proposed method and the traditional MOD method. Moreover, the computational resources are listed in Table II.

IV. CONCLUSION

A novel MOD solver is proposed to analyze the transient multiscale EM scattering problems. The whole computational region is divided into several subdomains, and each subdomain is enclosed with an ES. Then the interactions of the far-field subdomains are converted into the interactions of their corresponding ESs with BoR basis functions. Therefore, compared with the traditional MOD method, the memory requirement is reduced significantly and good convergence is obtained by the proposed method. Numerical examples are presented to demonstrate the validity and efficiency of the proposed method.

REFERENCES

[1] S. M. Rao, D. R. Wilton, and A. W. Glisson, "Electromagnetic scattering by surfaces of arbitrary shape," *IEEE Trans. Antennas Propagat.*, vol. 30, no. 3, pp. 409–418, May 1982.

[2] J. Song, C.-C. Lu, and W. C. Chew, "Multilevel fast multipole algorithm for electromagnetic scattering by large complex objects," *IEEE Trans. Antennas Propag.*, vol. 45, no. 10, pp. 1488–1493, Oct. 1997.

[3] M.-K. Li and W. C. Chew, "Multiscale simulation of complex structures using equivalence principle algorithm with high-order field point sampling scheme," *IEEE Trans. Antennas Propag.*, vol. 56, no. 8, pp. 2389–2397, Aug. 2008.

[4] F. Vipiana, M. A. Francavilla, and G. Vecchi, "EFIE modeling of high-definition multiscale structures," *IEEE Trans. Antennas Propag.*, vol. 58, no. 7, pp. 2362–2374, Jul. 2010.

[5] Z. Peng, X.-C. Wang, and J.-F. Lee, "Integral equation based domain decomposition method for solving electromagnetic wave scattering from non-penetrable objects," *IEEE Trans. Antennas Propag.*, vol. 59, no. 9, pp. 3328–3338, Sep. 2011.

[6] M. A. Francavilla, F. Vipiana, G. Vecchi, and D. R. Wilton, "Hierarchical fast MoM solver for the modeling of large multiscale wire-surface structures," *IEEE Antennas Wireless Propag. Lett.*, vol. 11, pp. 1378–1381, 2012.

[7] Z. Peng, K.-H. Lim, and J.-F. Lee, "Nonconformal domain decomposition methods for solving large multiscale electromagnetic scattering problems," *IEEE Trans. Antennas Propag.*, vol. 101, no. 2, pp. 298–319, Feb. 2013.

[8] B. Shanker, A. A. Ergin, K. Aygün, and E. Michielssen, "Analysis of transient electromagnetic scattering from closed surfaces using a combined field integral equation," *IEEE Trans. Antennas Propag.*, vol. 48, no. 7, pp. 1064–1074, Jul. 2000.

[9] Y.-S. Chung *et al.*, "Solution of time domain electric field integral equation using the Laguerre polynomials," *IEEE Trans. Antennas Propag.*, vol. 52, no. 9, pp. 2319–2328, Sep. 2004.

[10] B. Shanker, A. A. Ergin, M. Lu, and E. Michielssen, "Fast analysis of transient electromagnetic scattering phenomena using the multilevel plane wave time domain algorithm," *IEEE Trans. Antennas Propag.*, vol. 51, no. 3, pp. 628–641, Mar. 2003.

[11] A. E. Yilmaz, J.-M. Jin, and E. Michielssen, "Time domain adaptive integral method for surface integral equations," *IEEE Trans. Antennas Propag.*, vol. 52, no. 10, pp. 2692–2708, Oct. 2004.

[12] M.-D. Zhu, X.-L. Zhou, and W.-Y. Yin, "An adaptive marching-on-in-order method with FFT-based blocking scheme," *IEEE Antennas Wireless Propag. Lett.*, vol. 9, pp. 436–439, 2010.

[13] Q. Wang, Y. Shi, M. Li, Z. Fan, R. Chen, and M. Xia, "Analysis of transient electromagnetic scattering using UV method enhanced time-domain integral equations with Laguerre polynomials," *Microw. Opt. Technol. Lett.*, vol. 53, no. 1, pp. 158–163, 2011.

[14] H.-H. Zhang, Q.-Q. Wang, Y.-F. Shi, and R.-S. Chen, "Efficient marching-on-in-degree solver of time domain integral equation with adaptive cross approximation algorithm-singular value decomposition," *Appl. Comput. Electromagn. Soc. J.*, vol. 27, no. 6, pp. 475–482, 2012.

[15] W. Yu, D. Fang, and C. Zhou, "Marching-on-in-degree based time-domain magnetic field integral equation method for bodies of revolution," *IEEE Microw. Wireless Compon. Lett.*, vol. 17, no. 12, pp. 813–815, Dec. 2007.

[16] Z. He, H. H. Zhang, and R. S. Chen, "Parallel marching-on-in-degree solver of time-domain combined field integral equation for bodies of revolution accelerated by MLACA," *IEEE Trans. Antennas Propag.*, vol. 63, no. 8, pp. 3705–3710, Aug. 2015.

[17] Z. He, Z. H. Fan, D. Z. Ding, and R. S. Chen, "Solution of PMCHW integral equation for transient electromagnetic scattering from dielectric body of revolution," *IEEE Trans. Antennas Propag.*, vol. 63, no. 11, pp. 5124–5129, Nov. 2015.

[18] Z. H. Fan, Z. He, and R. S. Chen, "Marching-on-in-degree solution of the transient scattering from multiple bodies of revolution," *IEEE Trans. Antennas Propag.*, vol. 64, no. 1, pp. 321–326, Jan. 2016.

[19] M. G. Andreasen, "Scattering from bodies of revolution," *IEEE Trans. Antennas Propag.*, vol. 13, no. 2, pp. 303–310, Mar. 1965.

[20] J. R. Mautz and R. F. Harrington, "Radiation and scattering from bodies of revolution," *Appl. Sci. Res.*, vol. 20, pp. 405–435, Jan. 1969.

[21] W. C. Gibson, *The Method of Moments in Electromagnetics*. London, U.K.: Taylor & Francis, 2008.

[22] T. Su, L. Du, and R. Chen, "Electromagnetic scattering for multiple PEC bodies of revolution using equivalence principle algorithm," *IEEE Trans. Antennas Propag.*, vol. 62, no. 5, pp. 2736–2744, May 2014.

[23] M.-K. Li, W. C. Chew, and L. J. Jiang, "A domain decomposition scheme based on equivalence theorem," *Microw. Opt. Technol. Lett.*, vol. 48, no. 9, pp. 1853–1857, 2006.

Zi He received the B.Sc. degree in electronic and information engineering from the School of Electrical Engineering and Optical Technique, Nanjing University of Science and Technology, Nanjing, China, in 2011, where she is currently pursuing the Ph.D. degree in electromagnetic fields and microwave technology.

Her current research interests include antenna, RF integrated circuits, and computational electromagnetics.

Ru-Shan Chen (M'01–SM'15) was born in Jiangsu, China. He received the B.Sc. and M.Sc. degrees from the Department of Radio Engineering, Southeast University, Nanjing, China, in 1987 and 1990, respectively, and the Ph.D. degree from the Department of Electronic Engineering, City University of Hong Kong, Hong Kong, in 2001.

He joined the Department of Electrical Engineering, Nanjing University of Science and Technology (NJUST), Nanjing, where he became a Teaching Assistant in 1990 and a Lecturer in 1992. Since 1996, he has been a Visiting Scholar with the Department of Electronic Engineering, City University of Hong Kong, first as a Research Associate, then as a Senior Research Associate in 1997, a Research Fellow in 1998, and a Senior Research Fellow in 1999. In 1999, he was a Visiting Scholar with Montreal University, Montreal, QC, Canada. In 1999, he was promoted to Full Professor and Associate Director of the Microwave and Communication Research Center with NJUST, where he was appointed as the Head of the Department of Communication Engineering in 2007. He was also appointed as the Dean of the School of Communication and Information Engineering with Nanjing Post and Communications University, Nanjing, in 2009, and as the Vice Dean of the School of Electrical Engineering and Optical Technique with NJUST in 2011. He is currently a Principal Investigator of more than ten national projects. He has authored or co-authored over 260 papers, including over 180 papers in international journals. His current research interests include computational electromagnetics, microwave integrated circuit and nonlinear theory, smart antenna in communications and radar engineering, microwave material and measurement, and RF integrated circuits.

Prof. Chen is a member of the Electronic Science and Technology Group, a fellow of the Chinese Institute of Electronics (CIE), the Vice President of the Microwave Society of CIE and the IEEE MTT/APS/EMC Nanjing Chapter, and an Associate Editor of the *International Journal of Electronics*. He was a recipient of the Foundation for China Distinguished Young Investigators by the China NSF, a Cheung Kong Scholar of the China Ministry of Education, and the New Century Billion Talents Award. He received several best paper awards fro the national and international conferences and organizations. He serves as the Reviewer for many technical journals, such as the IEEE TRANSACTIONS ON ANTENNAS AND PROPAGATION, the IEEE TRANSACTIONS ON MICROWAVE THEORY AND TECHNIQUES, and *Chinese Physics*.

Wei E. I. Sha (M'09) received the B.S. and Ph.D. degrees in electronics engineering from Anhui University, Hefei, China, in 2003 and 2008, respectively.

He was a Postdoctoral Research Fellow with the Department of Electrical and Electronic Engineering, University of Hong Kong, Hong Kong, from 2008 to 2012, where he is currently a Research Assistant Professor. He engages in theoretical and computational research on electromagnetics and optics, focusing on the multiphysics and interdisciplinary research. The research topics are inspired by applications in several areas, including solar energy, microwave/optical communication, sensing/detection, and quantum information. He has co-authored two books, respectively, on wavelet theory and finite-difference time-domain method. He has authored 70 peer-reviewed journal papers in the Web of Science Core Collection. He also contributed to four book chapters at Springer, CRC Press, and InTech publishers. His current research interests include fundamental and applied aspects in plasmonics, emerging photovoltaics, metasurfaces, quantum electrodynamics, and computational electromagnetics.

Dr. Sha is a member of OSA. He received the Second Prize and First Prize of National Postgraduates Mathematical Contest in Modeling, respectively, in 2006 and 2007, and the Chinese Youth Science and Technology Innovation Prize in 2007. He and his collaborators received the Research Output Prize at the University of Hong Kong in 2013. In 2015, he received the Second Prize of Natural Science from the Anhui Province Government. He and his students received the Second Place of Best Student Paper at PIERS 2014, Guangzhou, China, the First Place of Best Student Paper at ACES 2014, Jacksonville, FL, USA, and the Best Student Paper at NCMMW 2015, Chongqing, China. In 2014, he received the Outstanding Reviewer of the *Journal of Computational Physics*. He served as a Committee Member or Session Chair of several international conferences, including PIERS 2016, Shanghai, China, ICCEM 2016, Guangzhou, IMWS-AMP 2015, Suzhou, China, EICT 2015, Khulna, Bangladesh, and ICSPS 2011, Yantai, China. He has been serving as the Reviewer of the IEEE, OSA, AIP, APS, and Nature Publishing Group journals. He served as the Book Proposal Reviewer for CRC Press and Bentham Science publishers.